# 3B5 SPECTRAL ANALYSIS OF DUAL-POLARIZATION RADAR SIGNALS IN A TORNADIC SUPERCELL STORM

Yadong Wang[1,2,*], Xiao Xiao[1,2], Tian-You Yu[1,2]

[1] School of Electrical and Computer Engineering, University of Oklahoma, Norman, Oklahoma, USA
[2] Atmospheric Radar Research Center, University of Oklahoma, Norman, Oklahoma, USA

## 1. INTRODUCTION

The upgrade of the Weather Surveillance Radar-1988 Doppler (WSR-88D) to dual-polarization is underway. The additional polarimetric variables can provide the insight of the scatterers' shape, size, and orientation, which can be used for retrieving drop size distribution, classifying the hydrometeors types, and improving rainfall estimation [e.g., Ryzhkov and Zrnic, 1998; Vivekanandan et al., 1999; Ryzhkov et al., 2000]. The polarimetric variables such as differential reflectivity ($Z_{DR}$) and cross correlation coefficient ($\rho_{hv}$) are typically estimated in the time domain, which provide integrated information of scatterers within the radar volume [Doviak and Zrnić, 1993]. Recently, several polarimetric signatures have been reported for several supercell storms using S-band radars, which include tornado debris signature, $Z_{DR}$ arc and $Z_{DR}$ columns signatures etc [e.g., Ryzhkov et al., 2005; Caylor and Illingworth, 1987; Conway and Zrnić, 1993; Kumjian and Ryzhkov, 2008].

Using spectral analysis, the differential reflectivity and cross correlation coefficient can be revealed as a function of radial velocities [e.g., Kezys et al., 1993; Yanovsky et al., 2005; Bachmann and Zrnić, 2006]. Together with the Doppler spectra, they have the potential to simultaneously study the mircophysic and dynamics within the radar volume. The KOUN radar, operated by the National Severe Storms Laboratory (NSSL), is a research prototype of the dual-polarization WSR-88D. Its unique capability of continuously collecting volumetric level I time series data makes the investigation of spectral signatures in a supercell storm possible.

This paper is organized as follows.The spectral density of polarimetric variables is presented in section 2. An example of tornadic supercell storm observed by S-band KOUN radar will be provided in section 3, and the polarimetric spectra from several interesting regions are reported. Summary and future work are presented in section 4.

* *Corresponding author address:* Yadong Wang, University of Oklahoma, School of Electrical and Computer Engineering, University of Oklahoma, Norman, Oklahoma 73019; e-mail: wyd@ou.edu

## 2. REVIEW OF SPECTRAL SIGNATURES IN DUAL-POLARIZATION RADAR

For a polarimetric weather radar, in addition to radar reflectivity, radial velocity, and spectrum width, parameters of $Z_{DR}$, $\rho_{HV}$, and specific differential phase ($K_{DP}$) can be estimated. The microphysical properties such as the drop size distribution (DSD) and drop types can be further studied. The Doppler spectrum is a power-weighted distribution of scatters' radial velocities within the radar resolution volume. The $Z_{DR}$ and $\rho_{HV}$ at each velocity component are estimated from Doppler spectra at both polarizations and are termed $Z_{DR}$ spectrum and $\rho_{HV}$ spectrum:

$$Z_{DR}(v) = 10 \times \log_{10} \frac{\sum_{i=1}^{n} |s_{hh}^{(i)}(v)|^2}{\sum_{i=1}^{n} |s_{vv}^{(i)}(v)|^2} \quad (1)$$

$$\rho_{HV}(v) = \frac{\sum_{i=1}^{n} s_{hh}^{(i)}(v) s_{vv}^{(i)*}(v)}{\sqrt{\sum_{i=1}^{n} |s_{hh}^{(i)}(v)|^2 \sum_{i=1}^{n} |s_{vv}^{(i)}(v)|^2}} \quad (2)$$

Where $s_{hh}^{(i)}(v)$ and $s_{hh}^{(i)}(v)$ are the Fourier transform of complex received signal from gate $i$ at horizontal and vertical channels, respectively. The spectral coefficient $v$ corresponds to the radial velocity [Bachmann and Zrnić, 2006]. In this study, the storm properties (such as velocity and DSD) in a relative small region are assumed not varying too much from one radar volume to another one. Therefore, the $\rho_{HV}$ spectra estimated along frequency direction are approximated as the one obtained along range direction. Each $\rho_{HV}$ spectrum component $\rho_{HV}(v)$ is estimated using $n$ gates, where $i$ represents the adjacent gate. Due to the limited number of samples in this approximation, the variance is relative high. The same $n$ gates ($n = 4$ in this study) are used to

calculate the averaged power spectra and $Z_{DR}$ spectra, which can reduce the statistical fluctuations.

## 3. A TORNADIC SUPERCELL STORM ANALYSIS

A tornadic supercell storm occurred in central Oklahoma on 30 May 2004, and several tornadoes were produced by this storm [Bluestein et al., 2006]. Several interesting regions with significant polarimetric signatures have be identified and analyzed by Kumjian and Ryzhkov [2008]. The Doppler spectra and the polarimetric spectra are estimated using the level I time series data collected by the KOUN radar, and the results are represented in the following part.

### *3.1. Polarimetric Spectral Signature From Tornado/Mesocyclone Region*

Zrnić and Doviak [1975] have shown that tornado spectra can have wide and bimodal signatures that set them apart from other weather spectra. Spectra similar to white noise but with significant signal power can be observed in a tornadic region using numerical simulations and data collected by WSR-88D with operational setups [Yu et al., 2007]. Recently low $Z_{DR}$ and low $\rho_{hv}$ were reported as the tornado debris signatures by Ryzhkov et al. [2005]. The tornado debris is assumed to consist of randomly oriented particles with irregular shapes. The plan position indicator (PPI) of velocity from the elevation angles between $0.0^o$ to $2.5^o$ are presented in Fig. 1. The contour of reflectivity of 30 dB is delineated by white lines. The Doppler spectra and $Z_{DR}$ spectra within the white box are represented in Fig. 2 and Fig. 3, respectively. Generally, when a tornado is relative close to a radar, spectra with tornadic spectral signatures (TSS) [Yu et al., 2007] can be observed from the tornado. However, in this case, the tornado is far ($>$ 80 km) from the radar, the spectra with TSS not only come from tornado, but also from mesocyclone. Relative flat $Z_{DR}$ spectra are also observed in this case, and the $Z_{DR}$ spectra components fluctuate around 0 dB at each gate.

### *3.2. Polarimetric Spectral Signature From high $Z_{DR}$ region*

Two distinct regions with high $Z_{DR}$ are typically observed in a supercell storm: $Z_{DR}$ arc and $Z_{DR}$ column. Generally the $Z_{DR}$ arc occurs on the right edge of the forward-flank downdraft (FFD), and the height of large $Z_{DR}$ (as high as 4 - 5 dB) is lower than 1-2 km; the $Z_{DR}$ column usually is located on the periphery of the bounded weak echo region (BWER), and relative large $Z_{DR}$ ( higher than 2 dB) can be extended as high as 7 km in a tornadic supercell storm [Kumjian and Ryzhkov, 2008]. An example of $Z_{DR}$ arc and $Z_{DR}$ column from the 30 May 2004 tornadic supercell is represented in Fig. 4. The contour of reflectivity of 30 dB is delineated by white lines. The $Z_{DR}$ arc only occurs at the first two elevation angles, while the $Z_{DR}$ column can be observed from all four elevation angles.

#### 1) $Z_{DR}$ arc

Significant $Z_{DR}$ arc signature, which produced by the size sorting associated with vertical shear, has been observed from several supercell storms in Oklahoma [Kumjian and Ryzhkov, 2008]. Doppler spectra from $Z_{DR}$ arc in Fig. 4 were estimated by periodogram with von Han window. Averaged spectra from every 4 gates are presented in Fig. 5. Different color represents different elevation angles, and solid and dashed line represent the spectra from horizontal and vertical polarization channel, respectively.

It is apparent that Doppler spectra with duel-peak or relative flat top shape at lower elevation angles($\leq 0.5^O$), however only one peak remains at higher elevation angles ($\geq 1.5^O$ ). Yu et al. [2008] suggest that such a spectral signature could be produced by the strong shears and the reflectivity distribution in vertical direction. The spectra from the first two elevation angles show similar shape (dual peaks or flat top), and they are different from the spectra from the higher two. One hypothesis is that the height of strong vertical shear is relative low. That could be the reason that in $Z_{DR}$ arc, the height of high $Z_{DR}$ is very shallow, generally lower than 2 km.

The averaged $Z_{DR}$ spectra along 4 gates are presented in Fig. 6. In the $Z_{DR}$ spectra, the components with power values less than noise level are not displayed. Large $Z_{DR}$ values can be observed for almost all valid velocity components at the first two elevations, and start to decrease from the third elevation. Large rain drops could dominate the low elevation angles of this region, and small drops start to occurs at high elevation angles. The results are consistent with the hypothesis of $Z_{DR}$ arc proposed by Kumjian and Ryzhkov [2008].

#### 2) $Z_{DR}$ columns

The signature of $Z_{DR}$ columns in supercell has been reported by Caylor and Illingworth [1987]; Conway and

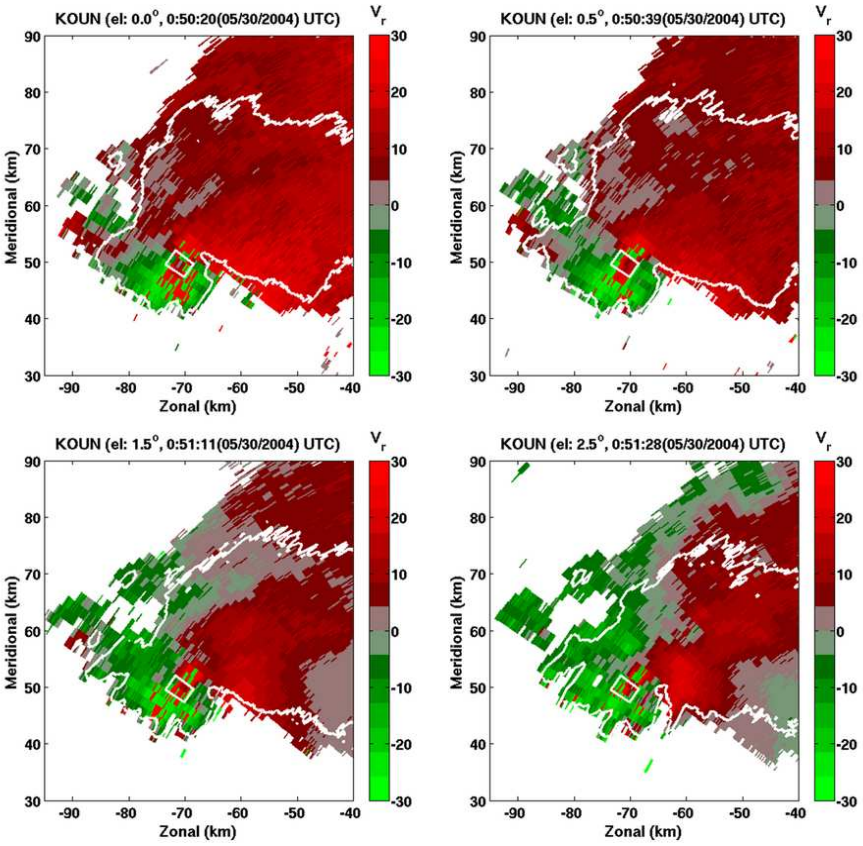


Figure 1: Velocity plot of the supercell storm on May 30 2004.

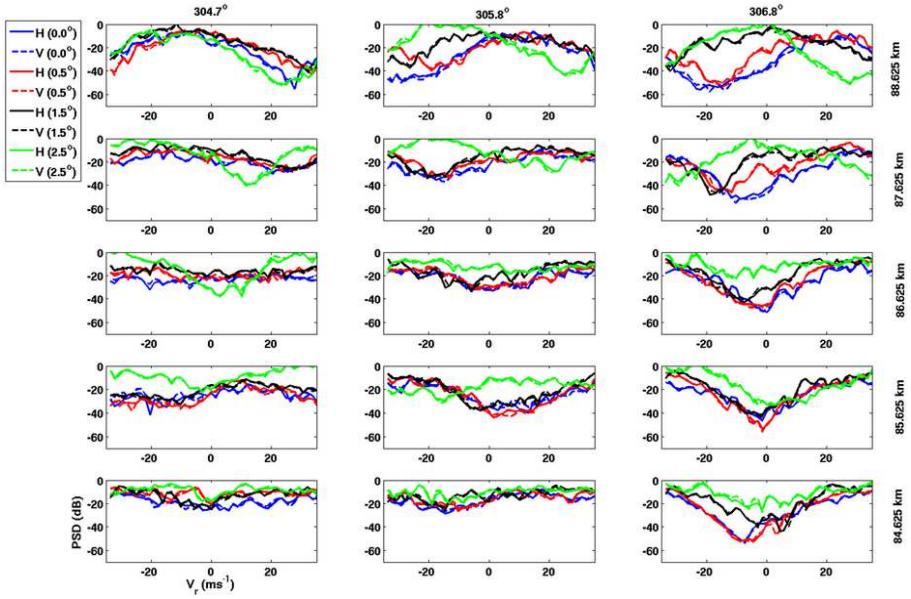


Figure 2: Doppler spectra from different elevation angles for a tornado case

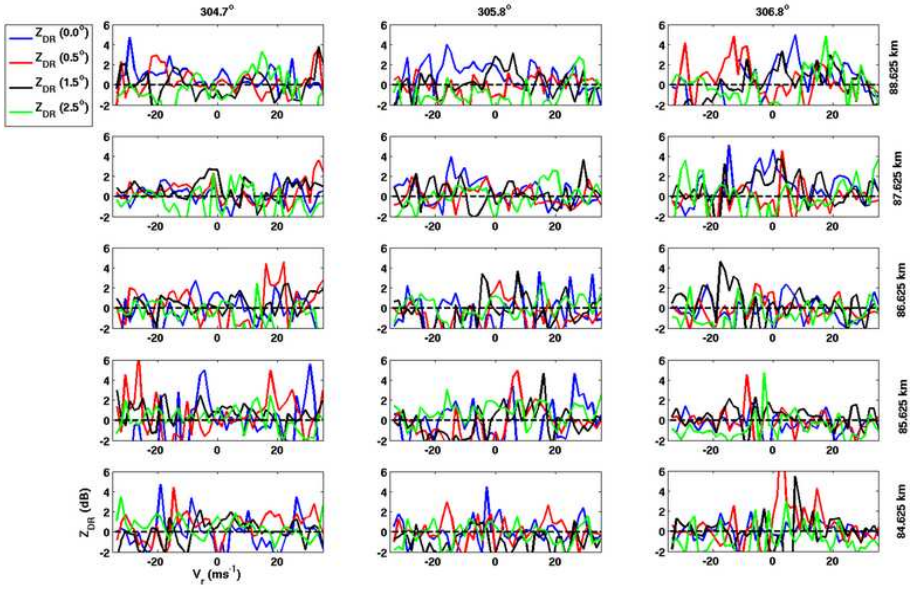


Figure 3: $Z_{DR}$ spectra from different elevation angles for a tornado case

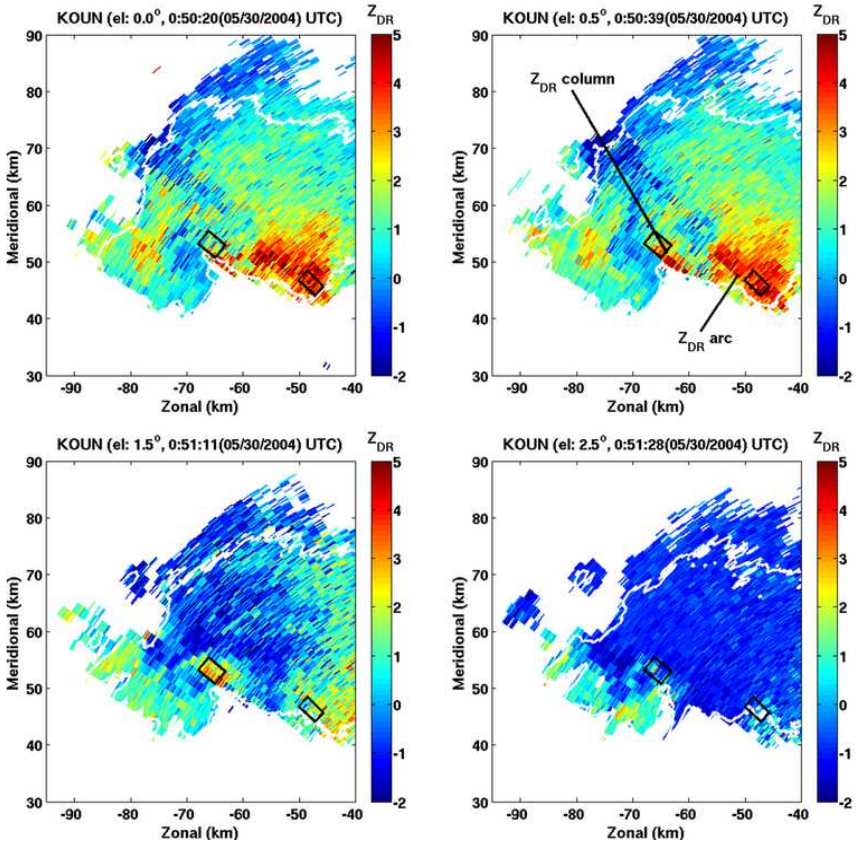


Figure 4: $Z_{DR}$ plots from different elevation angles. The regions within the black box are the portion of $Z_{DR}$ arc and $Z_{DR}$ column.

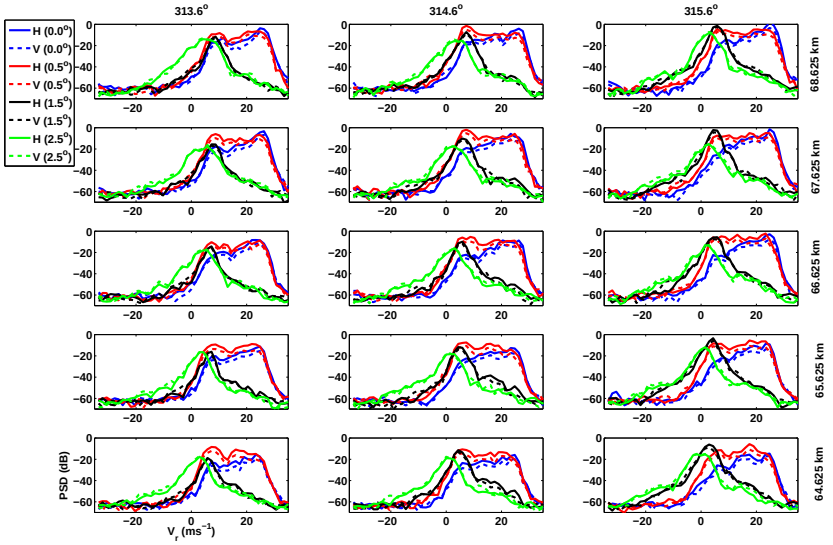


Figure 5: Doppler spectra from $Z_{DR}$ arc within the black box.

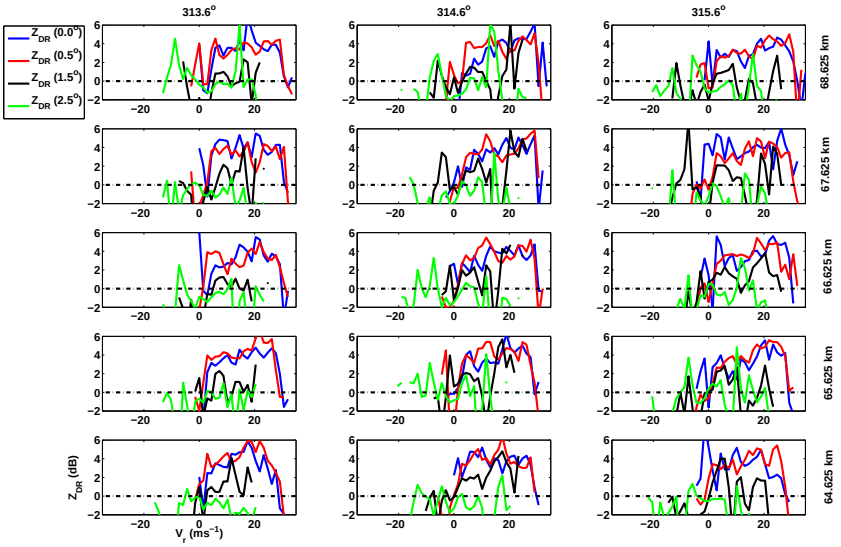


Figure 6: $Z_{DR}$ spectra from $Z_{DR}$ arc within the black box.

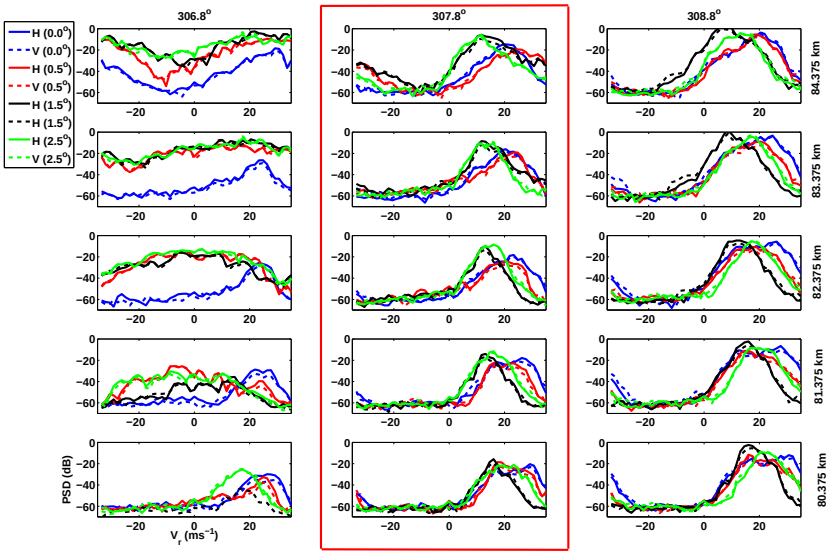


Figure 7: Doppler spectra from $Z_{DR}$ column within the black box.

Zrnić [1993]; Kumjian and Ryzhkov [2008]. The averaged spectra from $Z_{DR}$ column are presented in Fig. 7. Since the $Z_{DR}$ column is relative narrow, protruded $Z_{DR}$ only can be observed within the red frame. The spectra shapes show similarity at different elevation angles, even there could be some difference on the estimated mean velocity and spectral width. Different from the $Z_{DR}$ arc, the mechanisms produced the $Z_{DR}$ columns is mainly associated with thunderstorm updrafts instead of vertical shear. There is no abrupt spectral shape change from the first two elevation angles to the third and fourth.

The averaged $Z_{DR}$ spectra are presented in Fig. 8. At different elevation angle large $Z_{DR}$ value can be observed at almost all the velocity components. The $\rho_{hv}$ spectra at these two high $Z_{DR}$ regions show similar shape ( uniform value at all velocity components) and similar value ( $>$ 0.96 ), therefore are not shown in this paper.

### *3.3. Dual-polarization Spectral Signature From Wide-base Spectra Region*

Doppler spectra with wide-base signature are often observed from elevation angle of $1.5^o$ and higher in this tornadic supercell storm. The PPI of spectrum width from the elevation angles between $1.5^o$ to $4.5^o$ are presented in Fig. 9. The region with wide-base spectra is delineated by black lines, and it is partially overlapped with the $Z_{DR}$ arc. The contour of the reflectivity of 30 dB is delineated by white lines. Relative low spectral width ($<$ 3 m s $^{-1}$) and relative high reflectivity ( $>$ 30 dB) are other two signatures of this region. The range averaged spectra within the white box are presented in Fig. 10. From $1.5^o$ to $4.5^o$, these wide-base spectra continuously occur at different elevation angles, and exhibit similar shape and peak location. Each averaged spectrum can be divided into two part: the main peak, and the base. It is observed that the widths of both parts increase from low to high elevations. The $Z_{DR}$ and the $\rho_{hv}$ spectra within the white box are presented in Fig. 11 and Fig. 12, respectively. The $\rho_{hv}$ at peak parts show very high ($> 0.97$) values, which are close to the estimated value at time domain. However, at the base part, the $\rho_{hv}$ drops to as low as 0.8.

Different reasons could cause the decreasing of the integrated $\rho_{hv}$ within one radar volume, such as: distribution of eccentricities,differential phase shifts on scattering, sidelobes and receiver noise, etc. [e.g., Jameson, 1987; Balakrishnan and Zrnic, 1990; Doviak and Zrnić, 1993]. The variation of $\rho_{hv}$ at each velocity component has never been studied. This could be caused by the estimation method described in this work, or could be caused by any reasons described above, which worth more work to investigate.

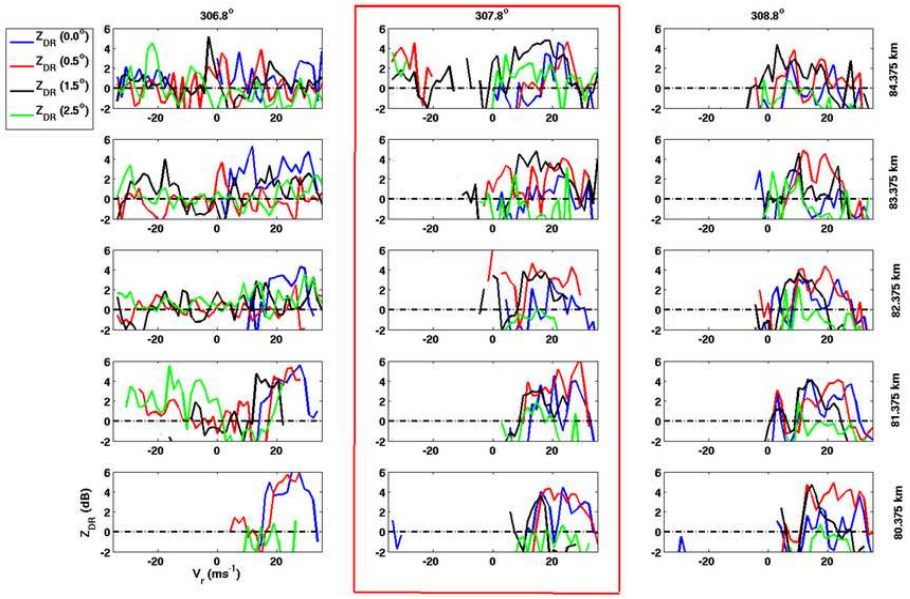


Figure 8: $Z_{DR}$ spectra from $Z_{DR}$ column within the black box

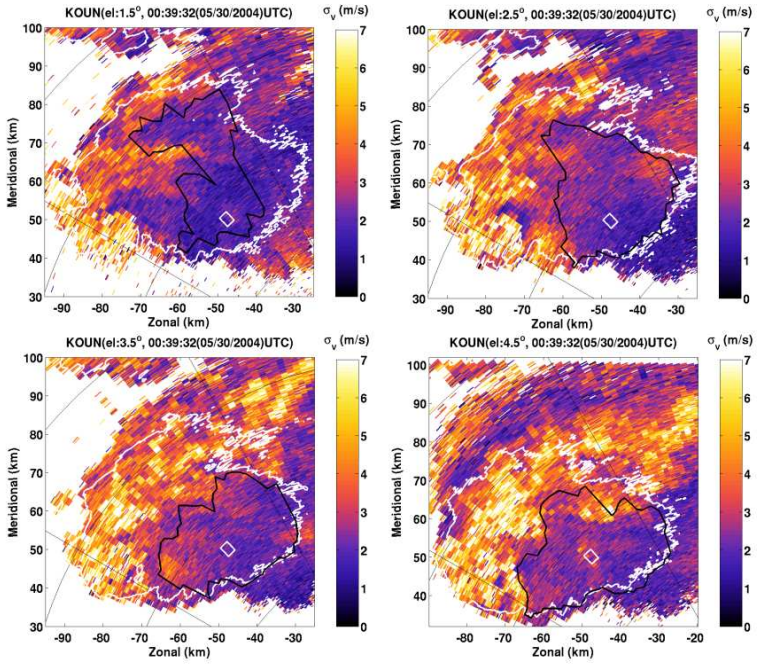


Figure 9: The spectrum width plot of the supercell storm on May 30 2004.

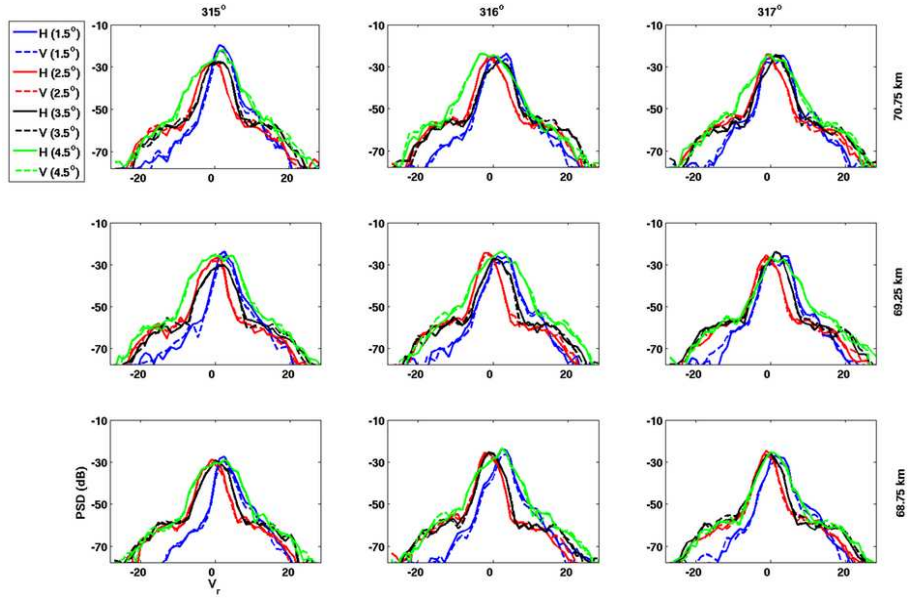


Figure 10: Doppler spectra from wide-base spectra region within the white box

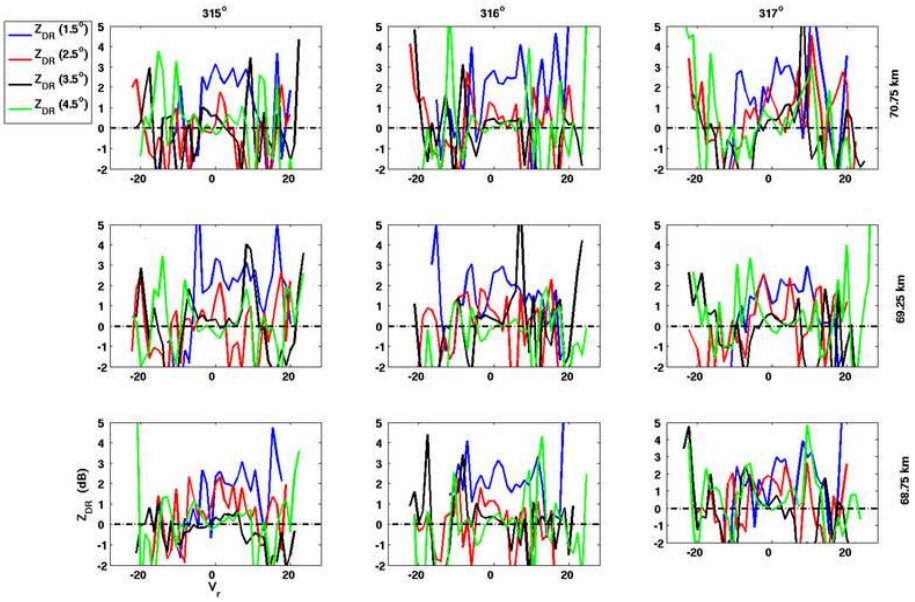


Figure 11: $Z_{DR}$ spectra from wide-based spectra region within the white box

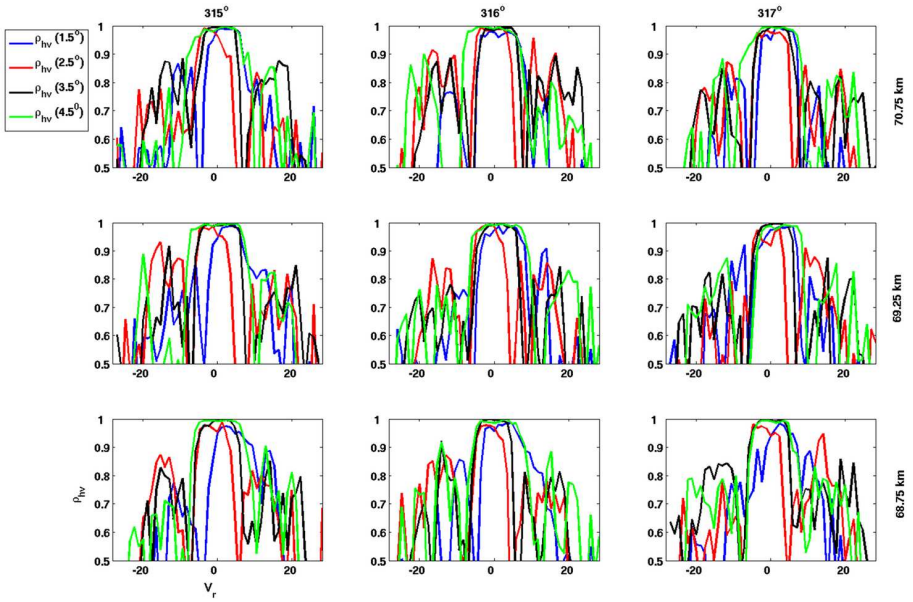


Figure 12: $\rho_{hv}$ spectra from wide-based spectra region within the white box

## 4. SUMMARY AND FUTURE WORK

Several interesting regions with significant polarimetric characters from a tornadic supercell storm are reported in this study. The polarimetric spectra from these regions are presented and discussed. More work is needed to further investigate the polarimetric spectral signature, and quantify the spectra at each location.

## 5. ACKNOWLEDGMENT

This work was primarily supported by the National Science Foundation through ATM-0532107. Any opinions, findings and conclusions or recommendations expressed in this material are those of the author(s) and do not necessarily reflect those of the National Science Foundation. The authors would like to thank all the help and comments from Dr. Alexander Ryzhkov and Mr. Matthew R. Kumjian. The authors would also like to thanks the NSSL staff for the collection of Level I data.

## References

Bachmann, S., and D. S. Zrnić, 2006: Spectral density of polarimetric variables separating biological scatterers in the VAD display. *J. Atmos. Oceanic Technol.*, **24**, 1186–1198.

Balakrishnan, N., and D. S. Zrnic, 1990: Use of polarization to characterize precipitation and discriminate large hail. *J. Atmos. Sci.*, **47**, 1525–1540.

Bluestein, H. B., M. M. French, and L. R. Tanamachi, 2006: Close-range observations of tornadoes in supercells made with a dual-polarization, X-band, mobile Doppler radar. *Mon. Weather Rev.*, **135**, 1522–1543.

Caylor, I. C., and A. J. Illingworth, 1987: Radar observations and modeling of warm rain initiation. *Quart. J. R. Met. Soc.*, **113**, 1171–1191.

Conway, J. W., and D. S. Zrnić, 1993: A study of production and hail growth using dual-Doppler and multiparameter radars. *Mon. Weather Rev.*, **121**, 2511–2528.

Doviak, R. J., and D. S. Zrnić, 1993: *Doppler Radar and Weather Observations*. Academic Press, San Diego, Calif., 130 pp.

Jameson, A. R., 1987: Relations among linear and circular polarization parameters meausured in canted hydrometeors. *J. Atmos. Sci.*, **4**, 634–645.

Kezys, V., E. Torlaschi, and S. Haykin, 1993: Potential capabilities of coherent dual polarization X-band radar. in *26$^{th}$ Conference on Radar Meteorology*, pp. 106–108, Norman, OK,. AMS.

Kumjian, M. R., and A. V. Ryzhkov, 2008: Polarimetric signatures in supercell thunderstorms. *J. Appl. Meteorol.*, **47**, 1940–1961.

Ryzhkov, A., and D. Zrnic, 1998: Discrimination between rain and snow with a polarimetric radar. *J. Appl. Meteorol.*, **37**, 1228–1240.

Ryzhkov, A., D. Zrnic, and R. Fulton, 2000: Areal rainfall estimates using differential phase. *J. Appl. Meteorol.*, **39**, 1341–1372.

Ryzhkov, A. V., T. J. Schuur, D. W. Burgess, and D. S. Zrnic, 2005: Polarimetric tornado detection. *J. Appl. Meteorol.*, **44**, 557–570.

Vivekanandan, J., D. S. Zrnic, S. M. Ellis, R. Oye, A. V. Ryzhkov, and J. Straka, 1999: Cloud mircophysics retrival using s-band dual-polarization radar measurements. *Bull. Amer. Meteor. Soc.*, **80**, 381–388.

Yanovsky, F., H. W. J. Russchenberg, and C. M. H. Unal, 2005: Retriveal of information about turbulence in rain by using Doppler-polarimetric radar. *IEEE Trans. Microwave Theory Technol.*, **53**, 444–450.

Yu, T.-Y., R. R. Rodiel, and R. D. Palmer, 2008: Investigation of non-gaussian weather spectra in a tornadic supercell. *J. Atmos. Oceanic Technol.*, **in press**.

Yu, T.-Y., Y. Wang, A. Shapiro, M. Yeary, D. S. Zrnic, and R. J. Doviak, 2007: Characterization of tornado spectral signatures using higher order spectra. *J. Atmos. Oceanic Technol.*, **24**, 1997–2013.

Zrnić, D. S., and R. J. Doviak, 1975: Velocity spectra of vortices scanned with a pulsed-Doppler radar. *J. Appl. Meteorol.*, **14**, 1531–1539.